Silver-Doped Cu_2SnS_3 Absorber Layers for Solar Cells Application

Jessica de Wild, Finn Babbe, Erika V. C. Robert, Alex Redinger, and Phillip James Dale

***Abstract*—The p-type semiconductor Cu_2SnS_3 is alloyed with Ag to investigate its effect on absorber layer and solar cell properties. Ag replaces the Cu in $(Cu_{1-x}Ag_x)_2SnS_3$ (ACTS) up to $x \leq 6\%$ at 550 °C. Above this percentage, Ag forms secondary phases. We find a significant increase in grain size, from hundreds of nanometers to several microns, and increased photoluminescence yield with increasing Ag concentration. Low-temperature photoluminescence measurements show that compensation is increased for the ACTS absorber layers, which could be beneficial for CTS, but also that the electrostatic band gap fluctuations are increased. The external quantum efficiency of the solar cells made from ACTS shows an increased carrier collection length from 320 nm for CTS to 700 nm and a thicker buffer layer. We attribute the increase in collection length to both increased depletion width (increased compensation) and diffusion length (larger grains). Overall the ACTS solar cells have a lower power conversion efficiency due to lower shunt resistance and open-circuit voltage, which are attributed to increase in pinholes, electrostatic fluctuation, and changes at the CdS/ACTS interface.**

***Index Terms*—Cu(In,Ga)S_2 (CIGS)/$Cu_2ZnSn(S,Se)_4$ (CZTS), heterojunctions, photoluminescence (PL), photovoltaic cell, thin films.**

I. Introduction

THE emerging material Cu_2SnS_3 (CTS) is a potential p-type absorber layer in thin film solar cells. It has a band gap of around 0.93 eV [1]–[5] and contains only earth-abundant elements similar to $Cu_2ZnSn(S,Se)_4$ (CZTS). Advantageously, it has fewer possibilities for secondary phases, defect complexes [6], and avoids the structural disorder arising with Cu/Zn exchange [7]. Solar cells made from CTS have reached an efficiency up to 4.6% synthesized from a NaF/Cu/Sn stacked precursor [8]. This is still far from the best CZTS efficiency of 12.6% [9] and several reasons are proposed for this deviation. The first reason is the structural disorder generated by local variations in the coordination of the Cu–Sn cations around S anions. CTS consists of two motifs, Cu_2Sn_2 and Cu_3Sn_1, periodically arranged and tetrahedrally bound to sulfur atoms [10]. Long range order of the motifs leads to the monoclinic structure and disorder to the cubic structure [11]. The disorder of the motifs is driven by entropy and may be unavoidable [12]. For CZTS, Cu/Zn disorder can shift the valence band up to 200 meV [7], while defect complexes involving Sn cause fluctuating conduction band edges of similar and even higher values [6]. Changes in band gap have neither been confirmed nor disproved for the disordered/ordered CTS polymorphs. However, theoretical calculations have shown that the cubic polymorph has several deep defects [11] and hence this phase should be avoided. This is also reflected in the performance of CTS solar cells, since the highest efficiencies are obtained from the monoclinic phase [1], [3]–[5] and consistent band gap values of (0.93 ± 0.02) eV with another optical transition at 1.00 ± 0.03 eV [1]–[5] are reported. The visible second transition is due to the splitting of the valence band and confirms the monoclinic polymorph [13], [14], but does not exclude the simultaneous presence of the cubic polymorph. Another potential problem with CTS is that the net doping is too high for good current extraction [11], [15]. Similarly to other copper chalcogenide semiconductors, the p-type doping is attributed to copper vacancies [16] and hence control of this is desirable. Baranowski *et al*. [11] found that the doping decreased several orders in magnitude when going from the cubic to monoclinic polymorph. They achieved a lowest doping level of 10^{17} cm^{-3} that is still rather high for good current extraction [17]. Theoretical calculations have shown that the defect formation energy of Cu vacancies is half of that of CZTS [18] and hence a high density of Cu vacancies is expected. Another way to control the doping is by compensating acceptors by adding donors. Based on the similar oxidation states of Cu and Ag, we propose to tackle the aforementioned problems by alloying CTS with Ag (ACTS). Alloying chalcopyrite materials with Ag has been shown to have several advantageous properties for kesterite and Cu(In,Ga)S_2 (CIGS) absorbers [19]–[26] [(Ag, Cu)$_2$ZnSnS$_4$ (ACZTS) and (Ag,Cu)(In,Ga)S_2 (ACIGS)]. Ag replaces Cu in these materials, which increases the band gap [19], [23], [24], [26], decreases the p-type doping [23], as well as reduces intragrain defects and defect states [19]–[21], [23], [26]. All these effects may be beneficial for CTS as well. First, the band gap of CTS is around 0.93 eV [1]–[5], which is lower than desired for single-junction solar cells. Second, a decrease of p-type doping when alloying with Ag is expected since the formation energy of Ag donor defects is lower than for acceptors for Ag_2ZnSnS_4 (AZTS) [19], and Ag may occupy Cu vacancies

Manuscript received June 21, 2017; revised August 2, 2017 and September 18, 2017; accepted October 13, 2017. The work of J. de Wild, E. V. C. Robert, and P. J. Dale was supported by the FNR funded through EATSS project no. C13/MS/5898466. The work of A. Redinger was supported by the FNR no. 7842175. *(Corresponding author: Jessica de Wild.)*

J. de Wild is with IMEC, Heverlee 3001, Belgium (e-mail: jessica.dewild@imec.be).

F. Babbe, E. V. C. Robert, A. Redinger, and P. J. Dale are with the Physics and Material Science Research Unit, University of Luxembourg, Belvaux L-4422, Luxembourg (e-mail: finn.babbe@uni.lu; erika.robert@uni.lu; alex.redinger@uni.lu; phillip.dale@uni.lu).

This paper has supplementary downloadable material available at http://ieeexplore.ieee.org.

Color versions of one or more of the figures in this paper are available online at http://ieeexplore.ieee.org.

Digital Object Identifier 10.1109/JPHOTOV.2017.2764496

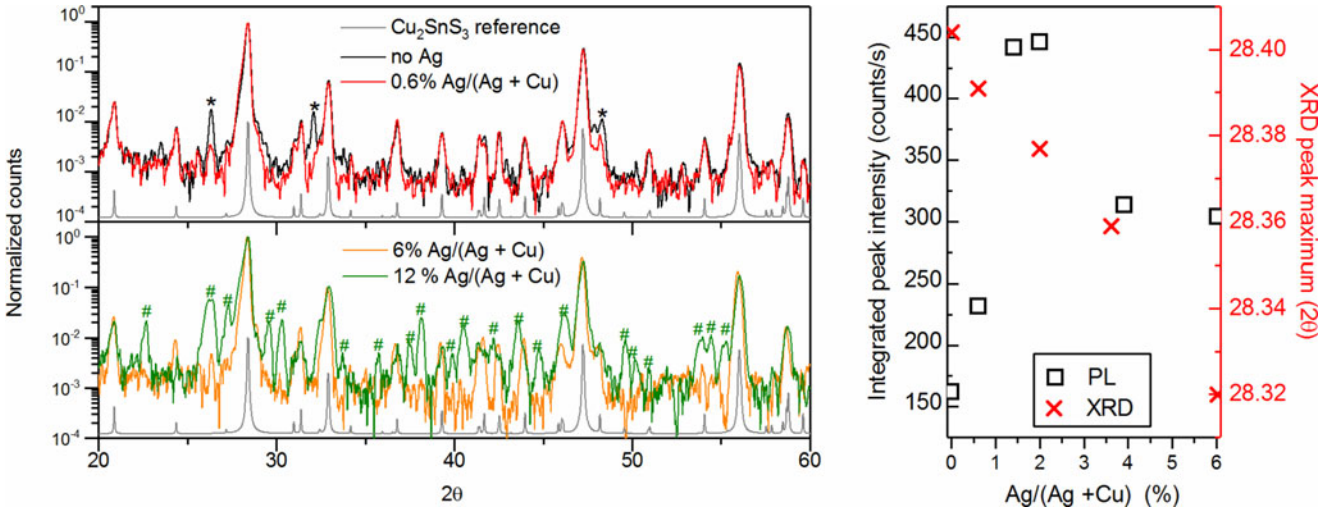

Fig. 1. Left: XRD diffractogram of pure CTS and ACTS with Ag/(Ag + Cu) of 0.6% (bottom), 6%, and 12% (top) as prepared. At higher than 6% Ag/(Ag + Cu), secondary phases # appear. CTS reference is plotted with Powdercell (c) (PDF 04-010-5719). The peaks marked with ∗ are related to Na_xCuSnS_3 [1]. Right: XRD peak shift of the main CTS peak at 28.40 and integrated PL yield dependence on the Ag concentration.

in ACZTS as well [22]. We expect the same effect for ACTS due to the similar chemistry and the fact that the Ag_2SnS_3 compound is n-type [27]. The last effect, i.e., reduction in intragrain defects, is especially beneficial for CTS since it is found that its planar defects increase the disorder and with that the deep defects [11]. Hence, Ag may reduce the deep defects in CTS via reduction of planar defects.

II. Experimental

To investigate the effect of Ag in CTS, ACTS absorber layers are prepared from Cu/Sn stacked precursors (400 nm each) sputtered on Mo/sodalime glass (SLG) via dc magnetron sputtering from high-purity metal targets. On top of the Cu/Sn stack, various thicknesses of Ag are deposited by ion beam sputtering from an Ag target (99.5%). Similar layers are prepared without the Ag layer to make pure CTS. The SLG/Mo/Cu/Sn/(Ag) stacks are then annealed at 550 °C for 30 min with a background pressure of 1 or 10 mbar $90\%N_2/10\%H_2$ in the presence of S and SnS powders. The latter is to avoid Sn losses and/or to add Sn via the SnS gas phase [28]. The resulting absorber layers are around 3 μm thick. Both CTS and ACTS absorber layers are characterized with grazing incidence-X-ray diffraction (XRD) (GI-XRD: $\theta = 0.6^\circ$ to 2.0°, Bruker D8, Cu $K_{\alpha(1+2)}$ X-ray source). Micrographs are recorded with a scanning electron microscope [Hitachi SEM (SU-70), 7 keV] and Cu/Ag/Sn/S compositions are measured by energy dispersive/wavelength dispersive X-ray (EDX/WDX) (Oxford instruments INCA X-MAX, 20 keV) on large areas ($120 \times 130\,\mu m^2$) and on points ($1\ \mu m^2$). Photoluminescence (PL) measurements were performed on all samples in a home-built setup (excitation wavelength 514 and 660 nm) at room temperature (RT-PL, 514 nm) and at 10 K (LT-PL, 660 nm). Devices are prepared following the SLG/Mo/(A)CTS/CdS/iZno/AZO configuration with Ni/Al front contacts. Potassium cyanide (KCN) etching is performed prior to CdS deposition. External quantum efficiency (EQE) and current density–voltage (*JV*) measurements were carried out in home-built setups. The *JV* light intensity was calibrated to be 100 mW/cm^2 with a calibrated silicon solar cell.

III. Results and Discussion

A. Structural and Morphological Properties of ACTS Absorber Layers

Fig. 1 (top left) shows the XRD pattern of a silver-free CTS film, i.e., 0% Ag/(Ag + Cu) crystallized in the monoclinic phase. This phase is accompanied with the secondary phase $Na_xCu_{1-x}SnS_3$, as explained in [1] and peaks attributed to this phase are assigned with ∗. For the ACTS sample with the lowest Ag/(Ag + Cu) ratio of 0.6%, we see that the peaks belonging to $Na_xCu_{1-x}SnS_3$ have virtually disappeared and only pure monoclinic ACTS is formed. This is a significant change for such a low amount of Ag. Apparently, Ag suppresses the formation of the Na compound. This can be expected based on its +1 valence and competition with Cu sites. While increasing the Ag concentration, we found that pure ACTS without any secondary phases was formed up to a concentration of Ag/(Ag + Cu) < 6% (see Supplementary Fig. S1.1). Higher concentrations of Ag lead again to the formation of secondary phases. This is shown in Fig. 1 (left below), and the peaks not matching CTS are assigned with #. The peaks with # could not be matched to any phase in the ICDD PDF 2016 database; however, we did find that they are removed with KCN etching (see Supplementary Fig. S1.2). EDX before and after etching showed that mostly Ag was removed, implying that these # phases contain Ag (see Supplementary Fig. S1.3). Unfortunately, etching away these secondary phases left large pinholes behind (Supplementary Figs. S1.4 and S1.5), making the layer unsuitable for solar cell application. Hence, the maximum Ag/(Ag + Cu) used in this study in the following experiments is 6%. Unidentified XRD reflections were also observed for ACIGS [20] and were also attributed to secondary phases. However, this happened for ACIGS with Ag/(Ag + Cu) > 50%, while in our experiments,

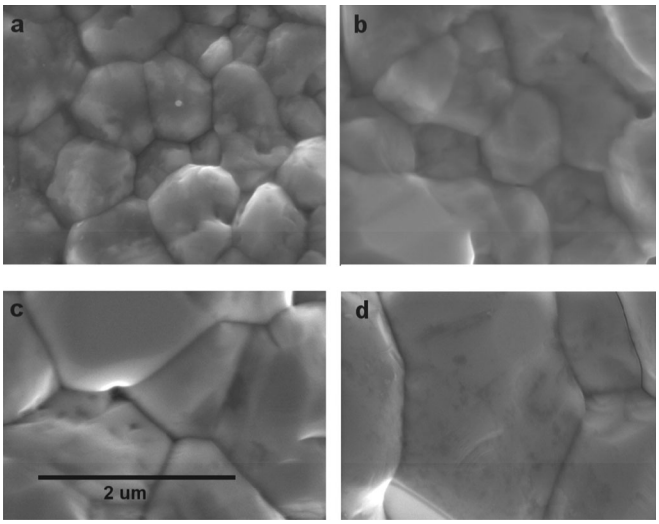

Fig. 2. SEM images for (a) 0.0%, (b) 0.6%, (c) 2%, and (d) 6% Ag/(Ag + Cu). Grains are increasing from less than 1 μm to several microns with increasing Ag(Ag + Cu) ratio. All micrographs have the same magnification.

it occurred already at 6%. This low solubility of Ag may be attributed to the fact that Ag_2SnS_3 crystalizes in another monoclinic space group (C2/c) than CTS (Cc) and replacing more Cu with Ag becomes energetically unfavorable as it wants to form another crystal structure. Despite this low concentration of Ag, significant changes are found. When Ag goes onto the Cu lattice sites, shifts of the XRD peaks to lower 2θ angles are expected. This is observed in our samples and shown on the right of Fig. 1. This shift is attributed to the increase of the lattice constant, due to the larger size of the Ag atom and therefore confirms the incorporation of Ag on Cu sites in the CTS lattice. The shift is not changing with increasing grazing incidence angle, i.e., X-ray penetration depth, from which we conclude that the Ag concentration is constant through the thickness of the layer (see Supplementary Fig. 2). A uniform distribution was also found for ACZTS [22]. Fig. 2 shows the SEM images for several ACTS layers with different Ag/(Ag + Cu) ratios. The apparent grain size increases from hundreds of nanometers to several microns. The effect of Ag on the intragrain defects and crystal growth is discussed for both ACZTS [22], [23], [25] and ACIGS [20]. Gershon *et al.* [23] and Su *et al.* [25] found largely increased grain size for ACZTS for a Ag/(Ag + Cu) ratio of $\sim$10%. For ACIGS [20] and ACZTS [22], it was shown that the number of planar defects is decreased. For ACIGS, the authors attributed this decrease to a lower melting point of the Ag compound, while for ACZTS, the authors attributed this decrease of planar defects to the filling the copper vacancies. Our changes are already observed for Ag/(Ag + Cu) ratios as low as 0.6% [compare Fig. 2(a) and (b)], which we speculate would not change the melting point significantly. Additionally, the chemistry of CTS is closer to that of CZTS and hence we believe the changes we found are due to the filling of copper vacancies.

B. Photoluminescence

RT-PL is performed on all samples under the same conditions to compare the PL yield of the different (A)CTS layers. The results are shown in Fig. 1 (on the right). With Ag, the PL yield is always higher than pure CTS and has a maximum at Ag/(Cu + Ag) = 2%. A higher PL yield indicates larger quasi-Fermi level splitting, which is a measure for V_{oc} [29]. Fig. 3 shows the normalized LT and RT-PL spectra for three samples: pure CTS (0% Ag), the highest PL yield [2% Ag/(Ag + Cu)], and the largest grains [6% Ag/(Ag + Cu)]. We see no positional peak shift of the maximum, implying that the band gap has not significantly changed with this low Ag incorporation. This is not so surprising, since the band gap of pure Ag_2SnS_3 is determined to be 1.26 eV [27]. At RT, the PL peak maximum is at 0.95 eV and is attributed to the conduction to valence band transition [1]. At lower energies, we see that the RT-PL yield is not going to zero, in agreement with our previous work [1], where we found that CTS has a large broad peak around 0.83 eV extending to the main transition. This 0.83 eV peak was mostly visible when the sample had signatures of the cubic phase [1]. The emission below 0.95 eV was attributed to tailing and defects belonging to the disordered cubic phase. It is seen though that the relative intensity for these defects/tail states lowers with increasing Ag concentration. This implies that incorporation of Ag results in a lower defect density and/or a more ordered compound.

Recently, defect transitions in CTS were examined by LT-PL [30], [31]. Several different donor to acceptor transitions were identified at 0.804, 0.840, and 0.865 eV. The individual peaks had slightly different *k*-values, activation energies, and blue shift per decade indicating that these are different defects. Unfortunately for CTS, lattice defects are not classified yet and hence they cannot be assigned to specific ones. For our samples, we see only one broad peak just below 0.81 eV, see Fig. 3. This peak is slightly broadened and red-shifted from 0.806 to 0.803 eV with increasing Ag/(Ag + Cu) ratio, as shown in the inset. The peak appearing below 0.78 eV is excluded, since it is at the edge of the detectors' sensitivity and hence the apparent peak maximum cannot be confirmed. Additionally, a peak at 0.93 eV emerges for higher Ag ratios and is visible in both the LT and RT-PL spectra, previously assigned to an exciton transition [31]. Since it is both visible in RT and LT spectra, we think it is also a defect transition. This hints to an increase of a certain defect in ACTS absorber layers, which is not directly related to the disordered cubic phase. From intensity-dependent LT-PL (see Fig. 3, on the right), we extract a blue shift of 1.7 meV/decade of the main peak around 0.8 eV for pure CTS, while the Ag samples give higher values of 3.5 and 4.1 meV/decade. This indicates an increase in compensation [32], which is what we expected and may be advantageous for solar cells. However, the broadening and red-shift of the defect peak may be attributed to increase in electrostatic fluctuations [32], which is bad for solar cell performance.

C. Devices

Solar cells are processed from ACTS absorber layers and compared with pure CTS absorber layers. All cells were processed the same way. Fig. 4 shows the *JV* curves of the best cells without Ag and with 4% Ag/(Ag + Cu). The power conversion efficiencies are 3% and 1%. The ACTS-based cell has a lower

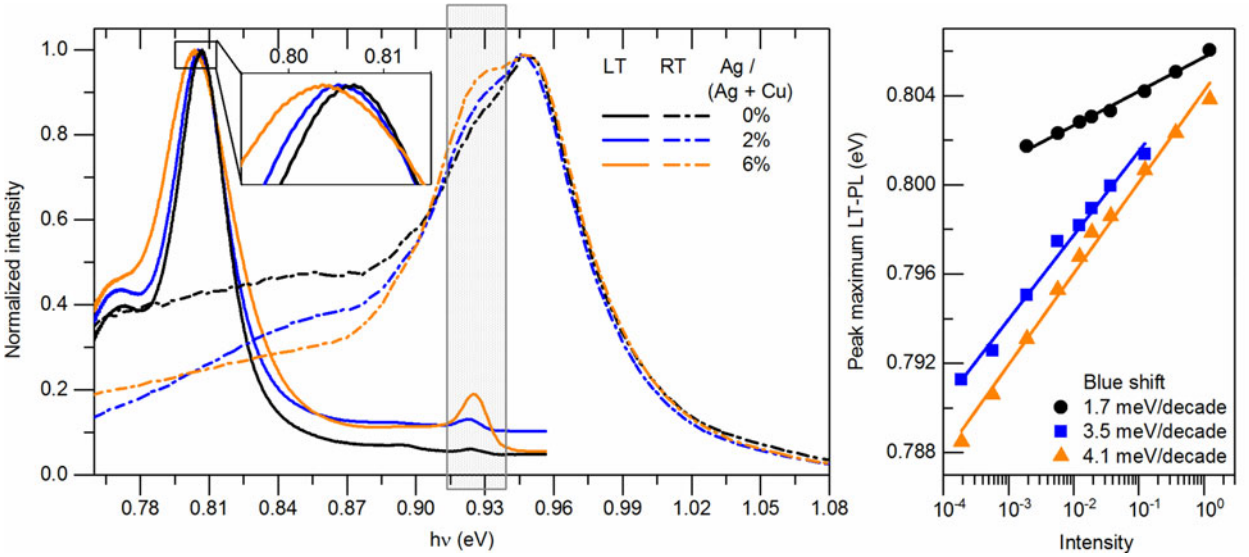

Fig. 3. Left: normalized RT-PL (dash lines) and LT-PL (solid lines). A small peak at 0.93 eV is visible in both RT and LT-PL. The inset shows a zoom image of the main LT-PL peak showing a red shift and broadening. Right: blue shift of the main peak with increasing laser power.

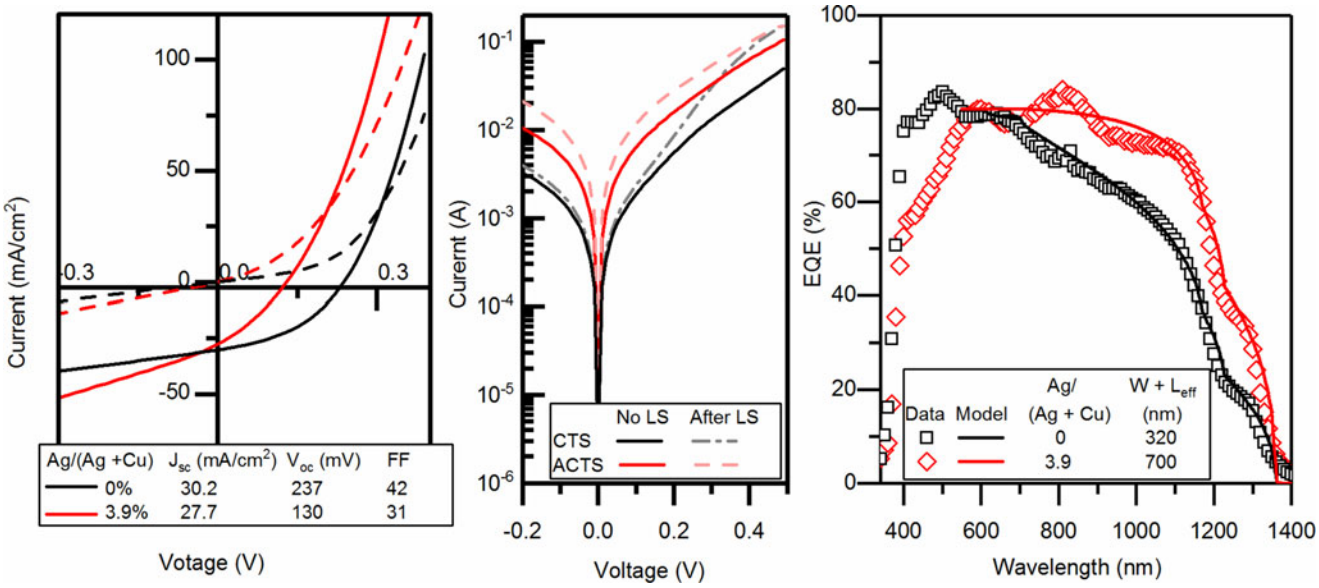

Fig. 4. Left: dark (dash) and light (solid) *JV* curves of the best cells without and with 4% Ag/(Ag + Cu). Middle: dark curves before and after light soaking (LS) Right: EQE of the two cells shows an increased collection length $W + L_{\text{eff}}$ for the Ag solar cells.

efficiency than the CTS solar cell due to a lower shunt resistance that causes a decrease in V_{oc}. The lower shunt resistance may be attributed to an increase in pinhole size and number, since on large area, larger pinholes were visible in the ACTS absorber (see Supplementary Material 3). Increase in pinholes or void formation can have many origins, such as having a bilayer structure with diffusion of one species into the other layer [33] and/or formation of secondary phases with volatile species [34]. Both are likely for the AgSnCu precursor, since Ag does not alloy with CuSn [35] leading to a bilayer structure and Sn forms volatile species at the annealing temperature used [28]. The increase of shunt paths we see in the ACTS absorber layers may be solved by changing the growth condition and/or the layer stacking. A decrease in V_{oc} can have various additional causes on top of the low shunt resistance. From low-temperature PL, we inferred that the potential fluctuations in the bulk material are increased, which is known to be bad for V_{oc} [36]. Another possible reason for the reduced V_{oc} could be changes at the CdS/ACTS interface. For ACIGS, it was found earlier that the defect concentration is increased at the CIGS/CdS interface, which could be reduced by light soaking (LS) [21]. To check whether the diode of our ACTS cells shows the same trend under LS as for ACIGS/CdS, dark curves were measured before and after 1 h of LS. The results are shown in Fig. 4 (in the middle). Interestingly, in our

case, it is the diode of CTS solar cells that has improved diode behavior, as can be seen from the dark current at positive bias voltage. The ACTS solar cell shows no improvement. It is even worsening the shunt resistance and there is barely any diode behavior left. Improvement of the diode under LS was also found for CZTS/CdS [37] and attributed to the removal of defects at the interface. There are several possibilities for this difference between ACTS and CTS. First, adding a new element, in this case silver, may add an interface defect; this was also found for the ACIGS/CdS interface [21]. Second, KCN etching has been shown to affect the surface band gap, leading to changes in recombination [38]. However, it is something that could be solved by optimizing the CBD parameters and/or add an etching step before the CdS deposition.

We see another difference concerning CdS when looking at lower wavelengths of the EQE, see Fig. 4 (on the right). The lower spectral response in this region can be attributed to a significantly thicker and/or more defective CdS layer on the ACTS absorber layer. This is another indication that the CdS growth is not the same on the CTS and ACTS absorbers, despite the same chemical bath synthesis. These differences could arise from reduced surface roughness of the ACTS surface due to the larger grains and/or increased nucleation of CdS onto the ACTS surface. From the shape of the EQE curves at higher wavelengths, it is clear that the effective collection length [depletion width (W) + diffusion length (L_{eff})] has drastically increased for the ACTS absorber. The EQE data for wavelengths longer than 540 nm were modeled with the formula $c{\cdot}(1 - \exp(-\alpha(W + L_{\text{eff}}))$, with c being a constant for parasitic absorption and interface recombination [15]. Details of the modeling procedure and absorption coefficient can be found in [13] and [15]. From the modeling, we determine an enhanced collection length ($W + L_{\text{eff}}$) from 320 to 700 nm for the ACTS solar cells. The thickness of the CdS layer itself has only minor influence on the current collection [36]. Hence, the enhanced collection length ($W + L_{\text{eff}}$) is likely due to an increased depletion width (W) due to a lower net doping in the absorber layer attributed to the higher compensation and increased diffusion length (L_{eff}) due to the larger grains.

Unfortunately, these advantages were canceled out by the problems previously mentioned: increased shunt paths and problems with the standard CdS deposition. Fortunately, both problems could be tackled by adapting the synthesis.

IV. Conclusion

We have shown that alloying CTS with Ag results in absorber layers with increased grain size and higher PL yield, which should be beneficial for solar cell performance. These changes are accompanied with increased electrostatic fluctuations. Devices prepared from ACTS have lower power conversion efficiencies than pure CTS. The main loss is a low shunt resistance due to increase in pinholes and reduced V_{oc}. Interestingly, there are no current losses due to increased effective carrier collection length in the ACTS absorber compared to CTS, implying overall beneficial absorber layer properties. Hence, it seems that the device structure is not optimized, and when the ACTS absorber layer is to be applied in solar cells, several aspects have to be taken care of. First, the number of shunt paths should be reduced. This may be possible by adapting the growth of the absorber layer and/or use different layer stacking. Second, the efficiency is likely reduced further due to a defective/unoptimized CdS/ACTS interface. We see different effects of the diode upon LS, but also from EQE measurements, we noticed that the CdS layer is thicker on the ACTS surface, which has an impact on the performance as well. Both problems can be tackled by optimizing the deposition of the absorber layer and the CdS layer and/or add some etching steps prior to device processing.

Acknowledgment

T. Unold is acknowledged for using the sputter machine at Helmholtz-Zentrum Berlin. The authors thank M. Melchiorre for solar cell processing. Prof. S. Siebentriet, J. Sendler, and G. Rey are acknowledged for discussion on the PL data. The LIST is acknowledged for the use of the XRD, SEM/EDX, and ion beam sputter. The authors thank the referees for their helpful feedback.

References

[1] J. de Wild, E. V. C. Robert, B. E. Adib, D. Abou-Ras, and P. J. Dale, "Secondary phase formation during monoclinic Cu2SnS3 growth for solar cell application," *Sol. Energy Mater. Sol. Cells*, vol. 157, pp. 259–265, Dec. 2016.

[2] D. M. Berg *et al.*, "Thin film solar cells based on the ternary compound Cu2SnS3," *Thin Solid Films*, vol. 520, no. 19, pp. 6291–6294, Jul. 2012.

[3] R. Chierchia *et al.*, "Cu2SnS3 based solar cell with 3% efficiency," *Phys. Status Solidi C*, vol. 13, no. 1, pp. 35–39, Jan. 2016.

[4] A. Kanai, K. Toyonaga, K. Chino, H. Katagiri, and H. Araki, "Fabrication of Cu $_2$ SnS $_3$ thin-film solar cells with power conversion efficiency of over 4%," *Jpn. J. Appl. Phys.*, vol. 54, no. 8S1, Aug. 2015, Art. no. 08KC06.

[5] N. Aihara *et al.,* "Sulfurization temperature dependences of photovoltaic properties in Cu 2 SnS 3-based thin-film solar cells," *Jpn. J. Appl. Phys.*, vol. 53, no. 5S1, May 2014, Art. no. 05FW13.

[6] S. Chen, A. Walsh, X.-G. Gong, and S.-H. Wei, "Classification of lattice defects in the kesterite Cu2ZnSnS4 and Cu2ZnSnSe4 earth-abundant solar cell absorbers," *Adv. Mater.*, vol. 25, no. 11, pp. 1522–1539, Mar. 2013.

[7] J. J. S. Scragg *et al.,* "Cu–Zn disorder and band gap fluctuations in Cu2ZnSn(S,Se)4: Theoretical and experimental investigations," *Phys. Status Solidi B*, vol. 253, no. 2, pp. 247–254, Feb. 2016.

[8] M. Nakashima, J. Fujimoto, T. Yamaguchi, and M. Izaki, "Cu_2 SnS_3 thin-film solar cells fabricated by sulfurization from NaF/Cu/Sn stacked precursor," *Appl. Phys. Express*, vol. 8, no. 4, Apr. 2015, Art. no. 042303.

[9] W. Wang *et al.,* "Device characteristics of CZTSSe thin-film solar cells with 12.6% efficiency," *Adv. Energy Mater.*, vol. 4, no. 7, May 2014, Art. no. 1301465.

[10] Y.-T. Zhai *et al.,* "Structural diversity and electronic properties of Cu 2 Sn X 3 (X = S, Se): A first-principles investigation," *Phys. Rev. B*, vol. 84, no. 7, Aug. 2011, Art. no. 075213.

[11] L. L. Baranowski *et al.,* "Effects of disorder on carrier transport in Cu2sns3," *Phys. Rev. Appl.*, vol. 4, no. 4, Oct. 2015, Art. no. 044017.

[12] P. Zawadzki, A. Zakutayev, and S. Lany, "Entropy-driven clustering in tetrahedrally bonded multinary materials," *Phys. Rev. Appl.*, vol. 3, no. 3, Mar. 2015, Art. no. 034007.

[13] J. de Wild, E. Kalesaki, L. Wirtz, and P. J. Dale, "Valence band splitting in Cu2(Sn,Ge,Si)S3: Effect on optical absorption spectra," *Phys. Status Solidi RRL, Rapid Res. Lett.*, vol. 11, no. 2, Feb. 2017, Art. no. 1600410.

[14] A. Crovetto *et al.,* "Dielectric function and double absorption onset of monoclinic Cu2SnS3: Origin of experimental features explained by first-principles calculations," *Sol. Energy Mater. Sol. Cells*, vol. 154, pp. 121–129, Sep. 2016.

[15] J. de Wild, E. Kalesaki, E. V. C. Robert, and P. J. Dale, "Quantum efficiency measurements and modeling as tools to monitor air annealing of Cu2SnS 3 solar cells," *IEEE J. Photovolt.*, vol. 7, no. 1, pp. 268–272, Jan. 2017.

[16] J. Ma, S.-H. Wei, T. A. Gessert, and K. K. Chin, "Carrier density and compensation in semiconductors with multiple dopants and multiple transition energy levels: Case of Cu impurities in CdTe," *Phys. Rev. B*, vol. 83, no. 24, Jun. 2011, Art. no. 245207.

[17] R. Scheer and H. W. Schock, *Chalcogenide Photovoltaics: Physics, Technologies, and Thin Film Devices*. Hoboken, NJ, USA: Wiley, 2011.

[18] H. Nishihara, T. Maeda, A. Shigemi, and T. Wada, "First-principles study of defect formation in the photovoltaic semiconductor Cu2SnS3 for comparison with Cu2ZnSnS4 and CuInSe2," *Jpn. J. Appl. Phys.*, vol. 55, no. 4S, Mar. 2016, Art. no. 04ES08.

[19] Z.-K. Yuan *et al.,* "Engineering solar cell absorbers by exploring the band alignment and defect disparity: The case of Cu- and Ag-based kesterite compounds," *Adv. Funct. Mater.*, vol. 25, no. 43, pp. 6733–6743, Nov. 2015.

[20] J. H. Boyle, B. E. McCandless, G. M. Hanket, and W. N. Shafarman, "Structural characterization of the (AgCu)(InGa)Se2 thin film alloy system for solar cells," *Thin Solid Films*, vol. 519, no. 21, pp. 7292–7295, Aug. 2011.

[21] P. T. Erslev, J. Lee, G. M. Hanket, W. N. Shafarman, and J. D. Cohen, "The electronic structure of Cu(In1 − xGax)Se2 alloyed with silver," *Thin Solid Films*, vol. 519, no. 21, pp. 7296–7299, Aug. 2011.

[22] W. Li, X. Liu, H. Cui, S. Huang, and X. Hao, "The role of Ag in (Ag,Cu)2ZnSnS4 thin film for solar cell application," *J. Alloys Compd.*, vol. 625, pp. 277–283, Mar. 2015.

[23] T. Gershon *et al.,* "Photovoltaic materials and devices based on the alloyed kesterite absorber (AgxCu1–x)2ZnSnSe4," *Adv. Energy Mater.*, vol. 6, no. 10, May 2016, Art. no. 1502468.

[24] J. H. Boyle, B. E. McCandless, W. N. Shafarman, and R. W. Birkmire, "Structural and optical properties of (Ag,Cu)(In,Ga)Se2 polycrystalline thin film alloys," *J. Appl. Phys.*, vol. 115, no. 22, Jun. 2014, Art. no. 223504.

[25] Z. Su, W. Li, G. Asim, T. Y. Fan, and L. H. Wong, "Cation substitution of CZTS solar cell with >10% efficiency," in *Proc. 2016 IEEE 43rd Photovolt. Spec. Conf.*, 2016, pp. 0534–0538.

[26] E. Chagarov *et al.*, "Ag2ZnSn(S,Se)4: A highly promising absorber for thin film photovoltaics," *J. Chem. Phys.*, vol. 144, no. 10, 2016, Art. no. 104704.

[27] A. O. Fedorchuk *et al.,* "Synthesis and spectral features of Ag2SnS3 crystals," *Mater. Chem. Phys.*, vol. 135, nos. 2–3, pp. 249–253, Aug. 2012.

[28] E. K. V. Robert, J. de Wild, and P. J. Dale, "Reaction chemistry of group IV containing copper chalcogenide semiconductors Cu2MX3 (M = Sn, Ge and X = S, Se)," *J. Alloys Compd.*, vol. 695, pp. 1307–1316, 2017.

[29] F. Babbe, L. Choubrac, and S. Siebentritt, "Quasi fermi level splitting of Cu-rich and Cu-poor Cu(In,Ga)Se2 absorber layers," *Appl. Phys. Lett.*, vol. 109, 2016, Art. no. 082105.

[30] N. Aihara, K. Tanaka, H. Uchiki, A. Kanai, and H. Araki, "Donor-acceptor pair recombination luminescence from monoclinic Cu2SnS3 thin film," *Appl. Phys. Lett.*, vol. 107, no. 3, Jul. 2015, Art. no. 032101.

[31] N. Aihara, Y. Matsumoto, and K. Tanaka, "Exciton luminescence from Cu2SnS3 bulk crystals," *Appl. Phys. Lett.*, vol. 108, no. 9, Feb. 2016, Art. no. 092107.

[32] P. W. Yu, "Radiative recombination in melt-grown and Cd-implanted CuInSe2," *J. Appl. Phys.*, vol. 47, no. 2, pp. 677–684, Feb. 1976.

[33] C. Lei, A. Rockett, I. M. Robertson, W. N. Shafarman, and M. Beck, "Void formation and surface energies in Cu(InGa)Se2," *J. Appl. Phys.*, vol. 100, no. 7, Oct. 2006, Art. no. 073518.

[34] H. R. Jung *et al.,* "Phase evolution pathways of kesterite Cu2ZnSnS4 and Cu2ZnSnSe4 thin films during the annealing of sputtered Cu-Sn-Zn metallic precursors," *Sol. Energy*, vol. 145, pp. 2–12, Mar. 2017.

[35] "Ag-Cu-Sn phase diagram & computational thermodynamics." [Online]. Available: https://www.metallurgy.nist.gov/phase/solder/agcusn.html. Accessed on: Jul. 31, 2017.

[36] J. Mattheis, U. Rau, and J. H. Werner, "Light absorption and emission in semiconductors with band gap fluctuations—A study on Cu(In,Ga)Se2 thin films," *J. Appl. Phys.*, vol. 101, no. 11, Jun. 2007, Art. no. 113519.

[37] M. Neuschitzer *et al.,* "Optimization of CdS buffer layer for high-performance Cu2ZnSnSe4 solar cells and the effects of light soaking: Elimination of crossover and red kink," *Prog. Photovolt. Res. Appl.*, vol. 23, no. 11, pp. 1660–1667, Nov. 2015.

[38] M. Bär *et al.,* "Cliff-like conduction band offset and KCN-induced recombination barrier enhancement at the CdS/Cu2ZnSnS4 thin-film solar cell heterojunction," *Appl. Phys. Lett.*, vol. 99, no. 22, Nov. 2011, Art. no. 222105.

[39] H. Wilhelm, H.-W. Schock, and R. Scheer, "Interface recombination in heterojunction solar cells: Influence of buffer layer thickness," *J. Appl. Phys.*, vol. 109, no. 8, Apr. 2011, Art. no. 084514.

Authors' photographs and biographies not available at the time of publication.